

Wind tunnel testing of a Wind Turbine with the Telescopic Blades: the influence of step change in chord

Mustahib Imraan, Rajnish.N.Sharma and R.G.J. Flay

Department of Mechanical Engineering
 University of Auckland, Auckland 1142, New Zealand

Abstract

The concept of a wind turbine with telescopic blades has been analysed for rotor blade performance using a wind tunnel scale model. In particular a model turbine with a two-stage telescopic blade system with a chord ratio of 0.6 was tested and the influence of this step change as well as blade extension were analysed. It was found that the effect of blade step change is significant at all blade extensions tested – the key influence being that performance is reduced relative to a blade system without a step change. A maximum loss in performance of about 20% was found to exist at a blade extension that was equivalent to one root blade chord. It was also found that prediction models based upon the blade element momentum theory over predict rotor performance for the step change blade system. Correlations are proposed for telescopic blade with step change in the chord to account for the step change losses, and these are in good agreement with the experimental data.

Introduction

The power output of a wind turbine P_t depends upon its efficiency or power coefficient C_p , the swept area $A = \pi d^2/4$ given by the diameter of the turbine blades d , the density of air ρ and the wind speed v ,

$$P_t = C_p \frac{1}{2} \rho A v^3 \quad (1)$$

$$P_t = C_p \frac{\pi}{8} \rho d^2 v^3 \quad (2)$$

To improve the power output of a wind turbine, the turbine efficiency, C_p , could be enhanced. Betz law limits a wind turbine’s aerodynamic efficiency to no more than 59.3% [1]. After accounting for actual aerodynamic performance and efficiency losses in the gearbox and in the generator, the maximum achievable efficiency is approximately 52% [2]. State of the art wind turbines already have system efficiencies in the order of 50% [2] so there is little room for improvement in the performance from efficiency gains. A wind turbine will also produce more energy at a given site with a larger diameter rotor. However, the size of the rotor, and hence the wind turbines energy capture, are limited in order to avoid damaging mechanical loads. Increases in rotor diameter also come at the expense of higher system capital cost. Wind turbine designs are often tailored to specific site characteristics with low wind speed sites having larger rotors and high wind speed sites having smaller rotors for the same power rating. The limiting mechanical loads are always developed in high wind conditions at any site and it is in those winds that it would be desirable to have a smaller rotor. Currently, most wind turbines use fixed length blades. Various control strategies such as variable speed and pitch, flexible blades, teetered rotors, feathering and furling have been used to increase energy capture and reduce system load.

However, these control strategies are unable to limit loads during storm conditions when the rotor is parked. During a storm, the only technique for limiting loads is to reduce the rotor diameter and/or the tower height. There are no other technically feasible methods of reducing loads in stormy conditions.

A more recent concept [2-9] as shown in Figure 1, to improve the power output and the Annual Energy Production (AEP) of a wind energy conversion system (WECS) involves varying the rotor diameter, d , through the use of telescopic or variable length blades. Such a system is one of the future energy conversion technologies that have gained some interest around the globe. The concept of telescopic blade offers dramatic opportunities to improve a wind turbines energy capture and cost effectiveness by controlling the length of the blades and indirectly controlling the swept area as shown in Figure 2. When wind speeds are low, the telescopic turbine blades extend thus increasing the swept area “A” which captures more energy as compared with a fixed blade length turbine. Alternatively, when the wind speeds are high (above the rated speed) the telescopic blades could retract thus reducing the mechanical loading on the system.



Figure 1. Telescopic blade wind turbine [2]

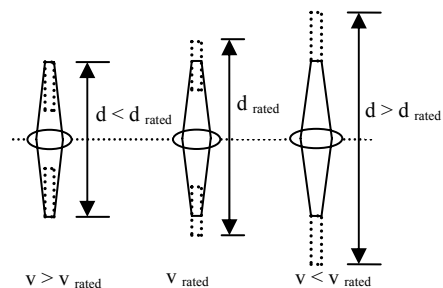


Figure 2. Telescopic wind turbine concepts

The performance characteristics of a telescopic blade horizontal axis wind turbine (TBHAWT) has been investigated in the wind tunnel for various tip speed ratios. In this study, the torque and rotor speed were measured for 3 different tip blade lengths being

equivalent to; $\frac{1}{2}$, 1 and 2 root blade chords i.e (~10, 20 and 40% of the root blade lengths). A symmetrical airfoil (NACA0018) with constant chord (70mm), 280mm long and no twist has been chosen for this research as it is simple and practical to fabricate. The chord ratio (Tip blade chord/Root blade chord) of 0.6 was chosen for structural strength reasons and ease of manufacture.

Experimental Setup and Procedure

Experimental tests as shown in Figure 3a were carried out at the 'Twisted Flow' wind tunnel facility at The University of Auckland. A uniform free stream is produced from an open type, recirculation system. The aluminium rotor blades were machined using the CNC and assembled to the hub (Figure 3b), which was mounted to a test rig enabling the measurement of torque and rotor rpm.

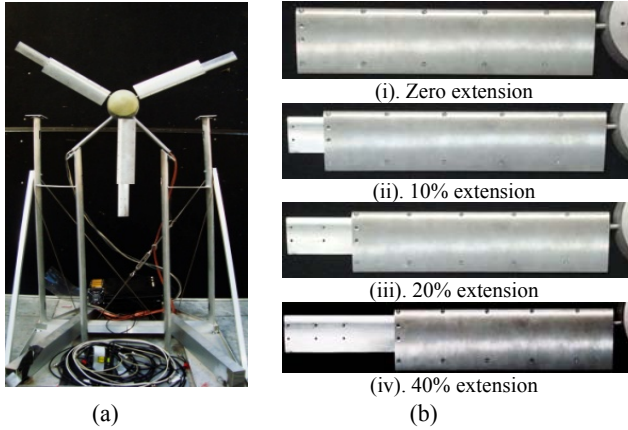


Figure 3. (a). Experimental setup. (b). Telescopic blade

Variations in power coefficients (C_p) versus tip speed ratio (λ) were studied. These parameters are generally defined by

$$\lambda = \frac{\omega R}{V} \quad C_p = \frac{T\omega}{0.5\rho AV^3} \quad (3)$$

where ω is the rotational speed (rad s^{-1}), R is the wind turbine radius (m), V is the inflow wind speed (m s^{-1}), T is the wind turbine torque (N m), ρ is the air density (kg m^{-3}) and A is the wind turbine disc area (m^2).

Rotor analysis using the Blade Element Momentum (BEM) method

Because of its simplicity, BEM theory has been the mainstay of the wind industry for predicting rotor performance. For this article, rotor performance predictions were acquired using a recent version of BEM theory, WT Perf [10]. One of the major limitations of the original blade element momentum theory is that there is no influence of vortices shed from the blade tips into the wake on the induced velocity field. These tip vortices create multiple helical structures in the wake. The effect of the wake on the induced velocity in the rotor plane is most pronounced near the tips of the blades, an area that also has the greatest influence on the power produced by the turbine.

Standard Blade

To compensate for this deficiency in BEM theory, a theory originally developed by Prandtl (see Glauert [11] and Vries [12]) may be applied. According to this method, a correction factor, F , is introduced into the thrust and torque equations. This correction factor is a function of the number of blades, the angle of the relative wind and the position on the blade.

Tip Loss

Prandtl simplified the wake of the turbine by modelling the helical vortex wake pattern as vortex sheets that are convected by the mean flow and have no direct effect on the wake itself. This theory is summarised by a correction factor to the induced velocity field, F_{tip} , and can be expressed by the following equation:

$$F_{tip} = \frac{2}{\pi} \cos^{-1} e^{-\left(\frac{B}{2} \left(\frac{R-r}{r \sin \phi}\right)\right)} \quad (4)$$

where B is the number of blade, R is the rotor radius, ϕ is the angle of relative wind and r is the radius anywhere along the blade as is shown in Figure 4. The tip loss correction factor characterizes the reduction in the force along the blade due to the losses at blade tip.

Hub Loss

Much like the tip loss model, the hub loss model serves to correct the induced velocity resulting from a vortex being shed near the hub of the rotor. The hub loss model uses a nearly identical implementation of the Prandtl tip loss model to describe the effect of this vortex:

$$F_{hub} = \frac{2}{\pi} \cos^{-1} e^{-\left(\frac{B}{2} \left(\frac{r-R_{hub}}{R_{hub} \sin \phi}\right)\right)} \quad (5)$$

where R_{hub} is the distance as shown in Figure 4.

The total loss due to hub and tip is given by [13, 14]

$$F = F_{tip} * F_{hub} \quad (6)$$

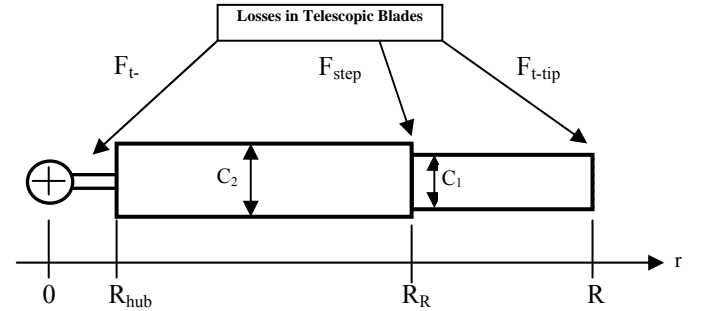


Figure 4. Telescopic Blade

Telescopic Blade

A correlation for blade losses due to the step change in the chord for the telescoping blade turbine is developed in this section. The concepts for the losses are similar to the standard blade losses but with an additional loss defined as step loss which is created by the introduction of a tip blade that has different chord length. With reference to Figure 4, the total loss at some radius r in the telescopic blade would be

$$F_{Telescopic} = F_{t-tip} * F_{t-hub} * F_{Step} \quad (7)$$

$$\text{where } F_{t-tip} = \frac{2}{\pi} \cos^{-1} e^{-\left(\frac{B}{2} \left(\frac{R-r}{r \sin \phi}\right)\right)} \quad (8)$$

$$\text{and } F_{t-hub} = \frac{2}{\pi} \cos^{-1} e^{-\left(\frac{B}{2} \left(\frac{r-R_{hub}}{R_{hub} \sin \phi}\right)\right)} \quad (9)$$

where $F_{Telescopic}$ is the total loss, F_{t-tip} is the tip loss, F_{t-hub} is the hub loss and F_{Step} is a loss for step. The latter is developed

by assuming two losses around the step, with a tip-type loss applied to the root blade, while a hub-type loss to the tip blade:

$$F_{Step} = F_{Step-tip} * F_{Step-hub} \quad (10)$$

$$F_{Step-tip} = \frac{2}{\pi} \cos^{-1} e^{-\left(\frac{B}{z} \left(\frac{R_R-r}{r \sin \phi}\right)\right)} \quad \text{for } R_{hub} \leq r \leq R_R \quad (11)$$

$$F_{Step-hub} = \frac{2}{\pi} \cos^{-1} e^{-\left(\frac{B}{z} \left(\frac{r-R_R}{R_R \sin \phi}\right)\right)} \quad \text{for } R_R \leq r \leq R \quad (12)$$

The step loss will be strongly dependent on the severity of the step change. Consider now the following special cases, where it is shown that for :

Case 1: if $c_1/c_2 = 1$, then $F_{Step} = 1$, therefore the overall blade loss would be

$$F_{Telescopic} = F_{t-tip} * F_{t-hub} \quad (13)$$

Case 2: if $c_1/c_2 = 0$, then $F_{Step} = 1$, therefore the overall blade loss would be

$$F_{Telescopic} = F_{step-tip} * F_{t-hub} \quad (14)$$

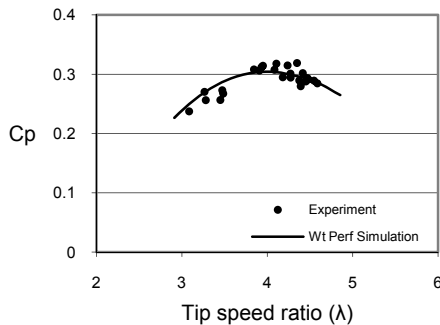
Case 3: if $0 < c_1/c_2 < 1$, then the overall blade loss would be

$$F_{Telescopic} = F_{t-tip} * F_{t-hub} * F_{Step} \quad (15)$$

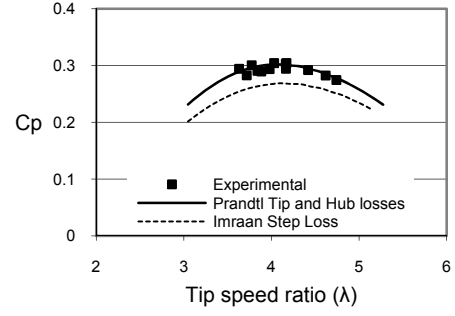
These codes were implemented in WT Perf.

Results and Discussion

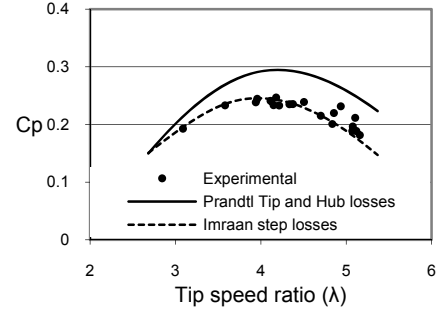
The variations in the power coefficients with respect to the tip speed ratio are shown in Figure 5. Performance parameter calculated using the computational procedure described above was compared with values obtained from the experimental study. As illustrated in Figure 5a, the predicted and experimental data for the blade with zero extension (refer Figure 3b(i)) is in good agreement. This was done in order to validate the experimental data with that of the WT Perf predicted data. The WT Perf simulation was carried out with the Prandtl tip and hub losses. Figure 5b shows the data for 10% blade extension. The experimental data agrees with the simulation with Prandtl tip and hub losses. The step losses correlation implemented in WT Perf over predicts the loss thereby reduces the power coefficient. However, for the blade with 20% extension, the experimental data as shown in Figure 5c agrees with the step loss model. The Prandtl tip and hub loss model over predicts the power coefficient. Similarly, the prediction for 40% extended blade as shown in Figure 5d, is closer to the step loss prediction model.



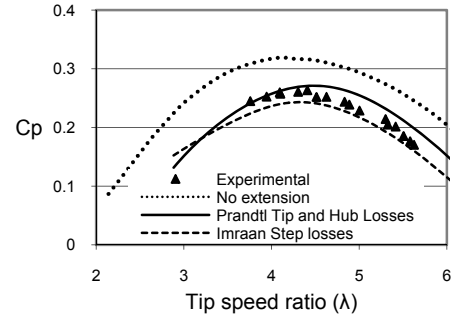
(a). Zero extension



(b). 10% extension



(c). 20% extension



(d). 40% extension

Figure 5. Experimental and predicted performance

The zero extension and the 10% extension blade have the highest power coefficient of approximately 0.3 at the tip speed ratio of ~ 4 . This suggests that 10% extension does not have significant impact on the step losses as the step change and the tip region more or less overlap each other. For blades with 20% extension, the power coefficient reduces by approximately 20% to 0.24 at tip speed ratio of ~ 4 . Similarly, for 40% extended blade, the power coefficient reduces by approximately 10% to 0.27.

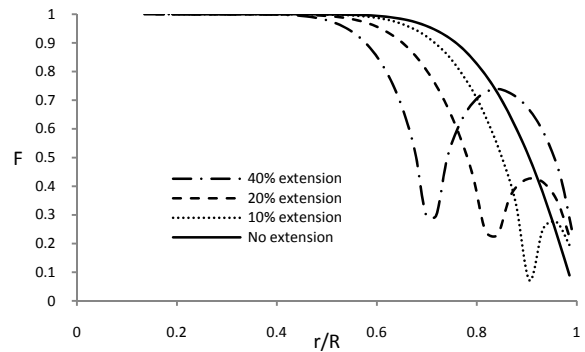


Figure 6. Blade correction factor as a function of radius for various extensions

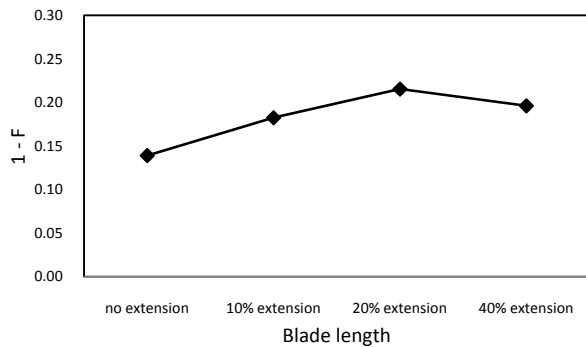


Figure 7. Blade loss factor as a function of blade extensions

Since the rotor radius is normalised, the area under the curves in Figure 6 represents the correction factor. For the blade with zero extension, the correction factor is maximum (or losses are minimum) when compared with a blade that has extension. From Figure 7, it is evident that the blade with zero extension has the minimum loss (1-F). For the blade with 20% extension, the step loss is highest against that of the 10% and 40% extended blade. It is also evident from Figure 6, that there exists a maxima in terms of step loss at 20% extension which is the extension equivalent to the root blade chord. Any change in the chord of the blade of a wind turbine causes the circulation to drop. As a result of the drop in circulation, vorticity is shed in the wake. The step change in chord for the tip blade has significant effect on the blade performance. For a very efficient blade, the correction factor will be close to unity.

For the blades tested, the lowest step change correction factor are 0.07, 0.23 and 0.3 for 10, 20 and 40% extensions. The 10% extended blade has the lowest correction factor at the step change region when compared with other extensions. It is likely that the wake generated due to the step change on the 10% extended blade overlaps with the tip vortices, thus the step loss is not significant and the tip loss dominates the losses. Hence the step loss prediction in Figure 6 demonstrates that the C_p values using tip and hub losses agrees with the experimental data. On the other hand, for the blade with 20% extension, the step change vortices and the tip vortices are likely separate to each other and have individual impact on the rotor performance. The additional step loss, to some extent deletes the lift contribution of the tip blade. Afjhe et al [15] showed similar explanation for tip controlled horizontal axis wind turbine performance. On the other hand, the 40% extended blade performance is 12.5% better than that of 20% extended blade. It is evident from Figure 6 that the step loss is also significant in this configuration but the blade extension is more than that of 20% therefore the lift contribution of the tip blade is considerable. Another reason for better performance of the 40% extended blade would be the aspect ratio of the tip blade higher than that of 20% extended blade therefore better lift to drag ratio.

Conclusions

A model turbine with a two-stage telescopic blade system with a chord ratio of 0.6 was tested and the influence of this step change as well as blade extension were analysed. It was found that the effect of blade step change is significant at all blade extensions tested – the key influence being that performance is reduced relative to a blade system without a step change. A maximum loss in performance of about 20% was found to exist at a blade extension that was equivalent to one root blade chord. It was also found that prediction models based upon the blade element momentum theory over predict rotor performance for the step change blade system. Correlations are proposed for telescopic

blade with step change in the chord to account for the step change losses, and these are in good agreement with the experimental data. Further investigations are underway.

Acknowledgments

This work was carried out in the framework of a PhD thesis supported by the University of Auckland, Auckland, New Zealand.

References

1. Manwell, J., J. McGowan, and A. Rogers, *Wind energy explained*. 2002, Chichester: Wiley. vii, 577.
2. Pasupulati, S.V., J. Wallace, and M. Dawson. Variable length blades wind turbine. in *Power Engineering Society General Meeting*, 2005. IEEE. 2005.
3. Dawson, H.M., *Variable Length Wind Turbine Blade*. 2006, Energy Unlimited Inc. <http://www.osti.gov/bridge/purl.cover.jsp?jsessionid=BFAD25BA636BD54E51E80FD6D341512?purl=/841190-OF8Frc/>.
4. McCoy, T.J. and D.A. Griffin, Control of Rotor Geometry and Aerodynamics: Retractable Blades and Advanced Concepts. *Wind Engineering*, 2008. **32**(1): p. 13-26.
5. Imraan, M., R.N. Sharma, and R.G.J. Flay. Telescopic Blade Wind Turbine to Capture Energy at Low Wind Speeds. in *Renewable Energy Asia – An International Conference & 4th Sustainable Energy and Environment Forum Meeting*. 2008. IIT Delhi, India.
6. Sharma, R.N. and U. Madawala, The Concept of a Smart Wind Turbine System, in *16th Australasian Fluid Mechanics Conference*. 2007: Crown Plaza, Gold Coast, Australia.
7. Sharma, R.N. and S. Berberich. Aerodynamic Analysis of a Wind Turbine with Telescopic Blades. in *25th AIAA Applied Aerodynamics Conference*. 2007. Miami, Florida.
8. Timothy, J.M. and A.G. Dayton, Active Control of Rotor Aerodynamics and Geometry: Status, Methods, and Preliminary Results., in *44th AIAA Aerospace Sciences Meeting and Exhibit*. 2006, AIAA 2006-605: Reno, Nevada.
9. Imraan, M., R.N. Sharma, and R.G.J. Flay. Telescopic blade wind turbines to capture energy at low wind speeds. in *ASME 3rd International Congress on Energy Sustainability*. 19-23 July, 2009. San Francisco, USA.
10. Marshall, L.B., *WT_Perf*. 2004, National Wind Technology Center - National Renewable Energy Laboratory, Golden, Colorado.
11. Glauert, H., "Airplane Propellers" *Aerodynamic Theory* (W.F. Durand, ed). 1935, Berlin: Springer Verlag.
12. Vries, O.D., *Fluid dynamic aspects of wind energy conversion*. 1979. p. Medium: X; Size: Pages: 150.
13. Moriarty, P.J. and A.C. Hansen, *AeroDyn Theory Manual*. 2005, National Renewable Energy Laboratory (NREL): Colorado, USA.
14. David J. Laino and A.C. Hansen, *AeroDyn User Guide*. 2002, Windward Engineering: Salt Lake City, Utah, USA.
15. Afjeh, A.A. and T.G. Keith, A simple computational method for performance prediction of tip-controlled horizontal axis wind turbines. *Journal of Wind Engineering and Industrial Aerodynamics*, 1989. **32**(3): p. 231-245.